Environmental Science and Pollution Research (2023) 30:83289–83301
https://doi.org/10.1007/s11356-023-28202-8

RESEARCH ARTICLE

Bacteria-based biochar as a persulfate activator to degrade organic pollutants

Na Yu[1] · Hanyu Ma[1] · Zhihong Wen[1] · Wenbin Zhang[1] · Jiahao Chen[1] · Yong Yuan[2] · Lihua Zhou[1]

Received: 15 November 2022 / Accepted: 6 June 2023 / Published online: 20 June 2023

Abstract

Carbon-based catalysts for activating persulfate to drive advanced oxidation processes (AOPs) are widely used in wastewater treatment. In this study, *Shewanella oneidensis* MR-1, a typical ferric reducing electroactive microorganism, was utilized as the raw material of biochar (BC) to prepare a novel green catalyst (MBC). The effect of MBC on activating persulfate (PS) to degrade rhodamine B (RhB) was evaluated. Experimental results showed that MBC could effectively activate PS to degrade RhB to reach 91.70% within 270 min, which was 47.4% higher than that of pure strain MR-1. The increasing dosage of PS and MBC could improve the removal of RhB. Meanwhile, MBC/PS can well perform in a wide pH range, and MBC showed good stability, achieving 72.07% removal of RhB with MBC/PS after 5 cycles. Furthermore, the free radical quenching test and EPR experiments confirmed the presence of both free radical and non-free radical mechanisms in the MBC/PS system, with •OH, $SO_4^{\bullet-}$ and $^1O_2$ contributing to the effective degradation of RhB. This study successfully provided a new application for bacteria to be used in the biochar field.

Keywords Biochar · *Shewanella oneidensis* MR-1 · Persulfate activation · Degradation · Rhodamine B

Introduction

Advanced oxidation process (AOP) is a new form of the advanced treatment of wastewater that has received much attention in recent years and is characterized by strong oxidation, rapid degradation, mild reaction conditions, and more thorough degradation of pollutants (Liu et al. 2020b; Sun et al. 2017, Wang and Wang 2021). Common AOPs include photocatalysis (Lai et al. 2019b; Li et al. 2018; Qin et al. 2019; Zhou et al. 2018), Fenton oxidation (Lai et al. 2019a), ozone oxidation (Levanov et al. 2019), persulfate activation (Li et al. 2022; Zeng et al. 2021; Zhu et al. 2023), and electrochemical oxidation (Zhang et al. 2019b). However, most of the oxidation methods in AOPs require large amounts of energy, complex operation, high cost, and harsh reaction conditions. Among them, the Fenton reaction process has a very wide pH range (2-4). The pH of the solution is too high or too low to effectively treat organic pollutants in wastewater. In contrast, PS is more friendly to the environment, easier to transport and store, and more stable in conventional environments. The PS can absorb energy or obtain an electron to generate $SO_4^{\bullet-}$, which can react further with water or hydroxide ions to generate •OH. In conventional methods, heat (Fan et al. 2015; Milh et al. 2021; Oh et al. 2009), UV-visible light (Ao et al. 2019; Lu et al. 2017), ultrasound (Monteagudo et al. 2018; Nasseri et al. 2017), transition metal ions (Fang et al. 2021; Wacławek et al. 2017; Wang et al. 2021a; Wei et al. 2016), and alkali can effectively activate PS to produce sulfate radical ($SO_4^{\bullet-}$) and hydroxyl radical (•OH). However, the several physical methods mentioned above generate high energy consumption. Transition metal ions need complex subsequent treatment to avoid secondary contamination. Alkali activation method needs to adjust the pH value, which is a risk of equipment corrosion (Fu et al. 2021; Shi et al. 2017; Wu et al. 2018). Therefore, it is necessary to explore more efficient and green activation methods.

Responsible Editor: Ricardo A. Torres-Palma

✉ Lihua Zhou
qhzhoulh@gdut.edu.cn

[1] School of Biomedical and Pharmaceutical Sciences, Guangdong University of Technology, Guangzhou 510006, China

[2] Guangdong Key Laboratory of Environmental Catalysis and Health Risk Control, School of Environmental Science and Engineering, Institute of Environmental Health and Pollution Control, Guangdong University of Technology, Guangzhou 510006, China

Carbon materials have broad applications in the field of catalysis due to their unique nanostructures, good electrical conductivity, chemical stability, and strong adsorption capabilities (Chen et al. 2021; Yu et al. 2020; Zhou et al. 2019). Carbon materials have been proven to be effective in activating PS by replacing various metals and metal oxides in various chemical processes. (Duan et al. 2016) found that phenol can be completely degraded after 150 min of reaction in the reduced graphene oxide rGO-900/PMS system. (Cheng et al. 2017) discovered that carbon nanotubes (CNTs) materials can effectively activate PS to produce singlet oxygen, thereby effectively degrading various pollutants. (Forouzesh et al. 2019) reported that oxidative degradation and adsorption jointly acted on the removal of metronidazole in the granular activated carbon (GAC)/PDS system, and PS efficiency was much higher than that of H_2O_2. However, the carbon-based materials mentioned above are generally expensive. In recent years, BC has been considered as an efficient carbon-based material for degrading organic pollutants due to its low cost, availability, ease of preparation, and recyclability of resources. It can be obtained by the pyrolysis of biomass feedstock under high temperatures and low oxygen conditions. Its morphological structures and physicochemical properties vary depending on the biomass and the pyrolysis process (Tag et al. 2016). Among them, metal-free BC materials exhibit non-metallic leaching properties, acid and alkali resistance, biocompatibility, recyclability and adaptability, and are promising and efficient catalysts (Chen et al. 2021; Yu et al. 2020). A series of studies have been undertaken on the activation performance of PS by using different types of metal-free biochar, such as sludge biochar (Huang et al. 2018, Wang and Wang 2019, Wu et al. 2021b, Yin et al. 2019), straw biochar (Duan et al. 2022; Feng et al. 2022; Tang et al. 2023; Wang et al. 2019a), wood biochar (He et al. 2019; Ouyang et al. 2019), algae biochar (Ho et al. 2019), shell biochar (Liang et al. 2019), and some biochar from waste (Chen et al. 2023; Zhao et al. 2022). BC from different biomass sources possesses different elemental compositions, surface structural properties, and redox capacities, which in turn affect their performance in PS activation efficiency. Thus, it is necessary to investigate the impact of the inherent properties of biomass on the performance of BC.

Microorganisms are the most biodiversity organisms on earth. They perform an essential role in the biosphere and provide mankind with numerous untapped resources. Especially bacteria have great potential for bio-decontamination in environmental pollution management (Timmis and Hallsworth 2022). Microorganisms can be used to degrade organic matters such as plastics (Zeenat et al. 2021) and toluene (Yan et al. 2020), and can also treat phosphates in industrial wastewater (Si et al. 2021) and sulfur-containing waste gasses, and can also help improve soil (Sanz et al. 2022). Recent years, the use of microorganisms in new directions has been studied. Liu et al. (Liu et al. 2021) investigated the different antioxidant capacities of *Lactobacillus plantarum* by crushing it with various methods such as high-pressure treatment (HIP), lysozyme combined with ultrasonic treatment (LCU), and freeze–thaw treatment (FAT). (Dong et al. 2022) investigated the effect of different forms of phosphate-solubilizing bacteria-*Paenibacillus xylanexedens* (bacterial supernatant, bacteria, broken bacteria) on *Chlorella pyrenoidosa*, providing a new approach to the treatment of wastewater. (Zhang et al. 2019a, 2021, 2022b) prepared novel and effective oxygen reduction reaction (ORR) electrocatalysts by crushing *Shewanella* cells through carbonization, electrostatic spinning-carbonization, and hydrogen reduction techniques. Based on the above research, we consider whether bacteria can be used as raw materials for the preparation of BC.

Using bacteria as precursor materials for the preparation of biochar, large surface areas and potentially controllable pore structures in carbon materials can be formed due to various highly porous cellular structures possessed by bacterial cells (Wei et al. 2015a, 2015b). Meanwhile, carbon materials with specific functions can be obtained from bacteria with the appropriate processing method (Guo et al. 2015). For example, (Wei et al. 2015b) synthesized heterogeneous carbon materials with nitrogen and phosphorus doping by direct carbonization using *Escherichia coli* (*E.coli*) as a precursor, and (Zhu et al. 2013) synthesized N-doped nanospheric particles with *Bacillus subtilis* by ion heating method. The electrochemically active bacterium, *Shewanella oneidensis* MR-1, is widely distributed in nature, and has low nutrient requirements, and can survive in common media (Yang et al. 2017; Zhang et al. 2009, 2022b). MR-1, as a Gram-negative facultatively anaerobic bacteria, consists of peptidoglycan, phospholipids, lipoproteins, and lipopolysaccharides, which can provide abundant heteroatoms for carbon materials. In addition, the outer membrane of MR-1 contains cytochrome c, a heme protein containing iron porphyrins, which is capable of electron transfer (Wu et al. 2023). (Hartshorne et al. 2007) reported that the iron porphyrin (Fe-N_4) on the outer membrane of MR-1 can be found to be transformed into Fe-N_x-C type active sites for ORR by pyrolysis. Therefore, in this work, *Shewanella oneidensis* MR-1 was first used as the precursor material of BC to evaluate the degradation effect of activated persulfate on organic pollutants.

Materials and methods

Experimental materials

Shewanella MR-1 was provided by the laboratory of the Guangdong University of Technology. rhodamine B (RhB), potassium persulfate (PS), hydrochloric acid (HCl),

and sodium hydroxide (NaOH) were obtained from Yung Man Biotech Co., Ltd. (Guangzhou China); methanol (MeOH, 99.0%), tert-butyl-alcohol (TBA, 99.0%), and sodium azide (NaN_3) were purchased from Sinopharm Chemical Reagent Co., Ltd. All chemicals utilized in this study were analytical grade.

Experimental procedure

The frozen MR-1 strain was first activated with beef paste peptone solid plate medium. Single colonies were then selected for enrichment in Luria–Bertani liquid medium (30°C, 150 rpm·min^{-1}), placed in a shaker and incubated aerobically for about 24 h to obtain the mother liquor.

The cultured MR-1 bacterial solution was centrifuged at 4℃ (6000 r·min^{-1}, 10 min) to settle the bacterium, removed the supernatant, and washed repeatedly with sterile saline more than three times to remove the residual medium, and then collected and dried at 60°C for 8 h in vacuum oven. Finally, solid particles/powder of MR-1 bacteria were collected and stored in a refrigerator at - 4℃. Subsequently, the dried MR-1 strain powder was placed in tube furnace (OTF-1200X, KeJing) for calcination. The temperature was raised to 700℃ for 4 h at a heating rate of 5℃·min^{-1} under the protection of nitrogen (N_2). After completion of the pyrolysis, the MR-1 powder sample was removed and washed several times with hydrochloric acid and then deionized water to neutralize to ensure complete removal of any residual inorganic ions. The washed samples were then dried in an oven at 65°C for 12 h to obtain MR-1 after carbonization (MBC).

RhB degradation experiments were performed in a brown conical flask with the beaker magnetically stirred (400 rpm) at ambient temperature. The initial pH of the reaction solution was adjustable using 0.1 M H_2SO_4 and 0.1 M NaOH. During the degradation of the system, a certain amount of MBC catalyst (0.2 g/L, 0.4 g/L, 0.6 g/L, 0.8 g/L) was added to 10 mg/L of RhB solution. Different concentrations of PS (2 mM, 4 mM, 6 mM, 8 mM) in the mixed solution were added to initiate the degradation reaction. The whole experiment was carried out under the condition of avoiding light. To measure the absorbance, the solution was collected at predetermined intervals and filtered through 0.22 μm filter. To evaluate the stability and reusability of the MBC, the reacted BC was washed repeatedly with ultrapure water and ethanol by means of filtration, followed by drying at 60°C, and then used for the next round of degradation experiments. The radical species in the MBC/PS system were determined using methanol (MeOH), tert-butyl alcohol (TBA), and sodium azide (NaN_3) as quenching agents. All trials were done in three parallel groups.

Analytical methods

The morphological changes before and after MBC reaction and the composition of micro-elements were analyzed by scanning electron microscopy (SEM, FEI INSPECT F50) and Energy Dispersive Spectrometer (EDS, Hitachi SU8100), respectively. Functional groups on the material surface were explored using a Fourier transform infrared spectrophotometer (FTIR, Nicolet 6700). A D8 Advance X-ray powder diffractometer (Bruker) was applied to study the crystalline structure of the BC material. The specific surface area and pore size distribution of the samples were determined by N_2 adsorption–desorption isotherms using a Brunauer-Emmett-Teller (BET, Micromeritics, 3-flex) at 77 K. RhB concentration was determined by ultraviolet spectrophotometry (UV-2600, Shimadzu). The EPR analysis was carried out with a Bruker EMXplus-10/12 spectrometer.

The degradation process of RhB in the MBC/PS system conforms to the pseudo-first-order kinetic model (Zhu et al. 2018b).

$$\ln C/C_0 = -k_{obs}t$$

where C_0 (mg/L) is initial RhB concentration, C (mg/L) is the concentration of RhB at a given time (min), and k_{obs} are the estimated pseudo-first-order rate constant (min^{-1}).

Results and discussion

Characterization of MBC

The morphology of *S. oneidensis* MR-1 and MBC were analyzed by SEM to compare the changes of pure bacteria and MBC before and after the reaction. As shown in Fig. 1a, MR-1 showed a rod-like shape with rough surface, but the bacteria were relatively intact, and the length of the bacteria was about 2–3 μm. It can be clearly seen from Fig. 1b-c that the morphology of MBC obtained by high-temperature calcination of MR-1 has changed greatly, showing irregular block structure and rich pore structure. Meanwhile, significant morphological differences are not observed for the MBC before and after the reaction. The mass ratio of MBC before and after heating at 700 °C for 4 h in a muffle furnace was used to calculate the ash content of MBC was 28.81% (Wang et al. 2019b). EDS energy spectrum in Fig. 1d showed that MBC contains the other elements of Na, K, P, Zn, Mg, Ca, and Al and the main elements of C, N, and O. Trace Fe was also found probably due to the existence of iron porphyrin on the outer membrane of MR-1. By comparing the specific surface area of MBC before and after the reaction, it can be observed that the specific surface area of the sample increased from 3.9933

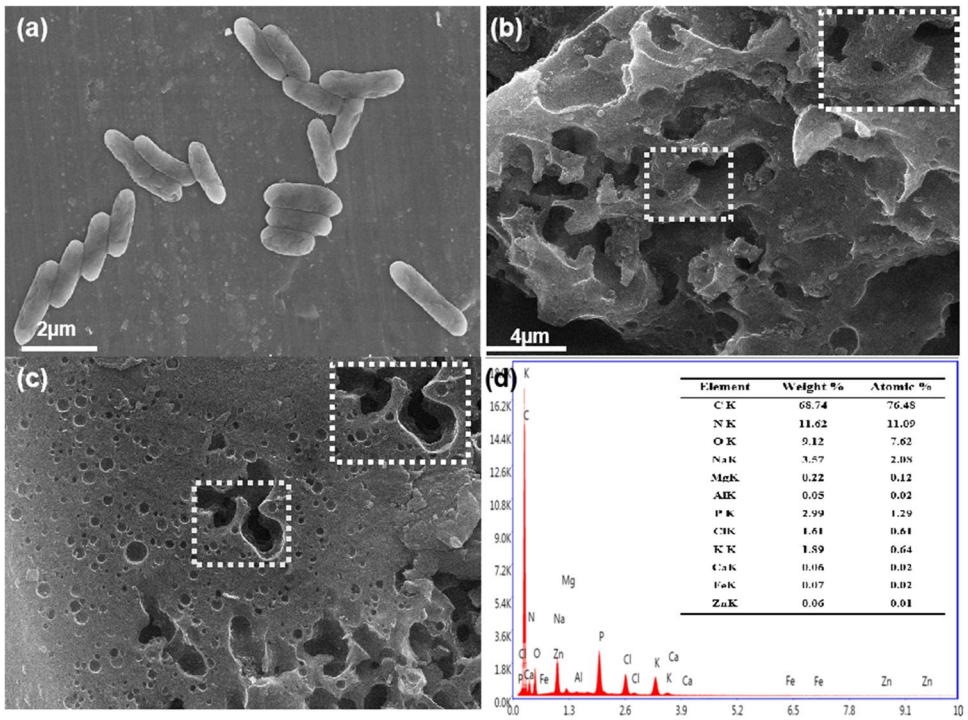

Fig. 1 SEM images of MR-1 (**a**), before (**b**) and after the reaction of MBC (**c**), and EDS spectra of MBC (**d**)

to 5.0058 m^2g^{-1} (Fig. 2a-b), which was estimated by the Brunauere-Emmette-Teller (BET) equation. It may indicate that MBC has no adsorption effect on RhB. Adsorption often shields the active center and hinders the electron transport process, thus affecting the catalytic performance (Liu et al. 2020a). Calculated by the Barrette-Joynere-Halenda (BJH) equation, the pore volume and average pore size of the MBC before and after the reaction were 0.0116 cm^3g^{-1}, 0.0118 cm^3g^{-1}, 11.5977 nm, and 9.3968 nm, respectively. It can be noticed that the isotherms of adsorption and desorption of MBC were not closed to result in a non-closed hysteresis loop, which can indicate the microporous structure of MBC. Furthermore, the average pore radius centered at 2 nm (Fig. 2c) could also indicate a homogeneous microporous structure in the MBC. It was reported that the uniform porous structure of BC can offer more active sites to favor the activation of PS (Zhao et al. 2022).

The XPS spectra of Fig. 3 provide a simple qualitative analysis of the main constituent elements of MBC. The wide-survey XPS spectra revealed three distinct distinctive peaks of C 1 s (284.30 eV, 47.03 at. %), N 1 s (399.18 eV, 5.49 at. %), and O 1 s (531.45 eV, 6.89 at. %). The C 1 s spectrum is shown in Fig. 3a and could be considered as the contents of C–C/C = C (284.8 eV), C-O (285.92 eV), and O-C = O (288.75 eV) (Kong et al. 2016; Shi et al. 2017; Wu et al. 2021b). The presence of elemental nitrogen can be divided into three forms (Fig. 3b), namely, pyridinic N (397.43 eV), graphitic N

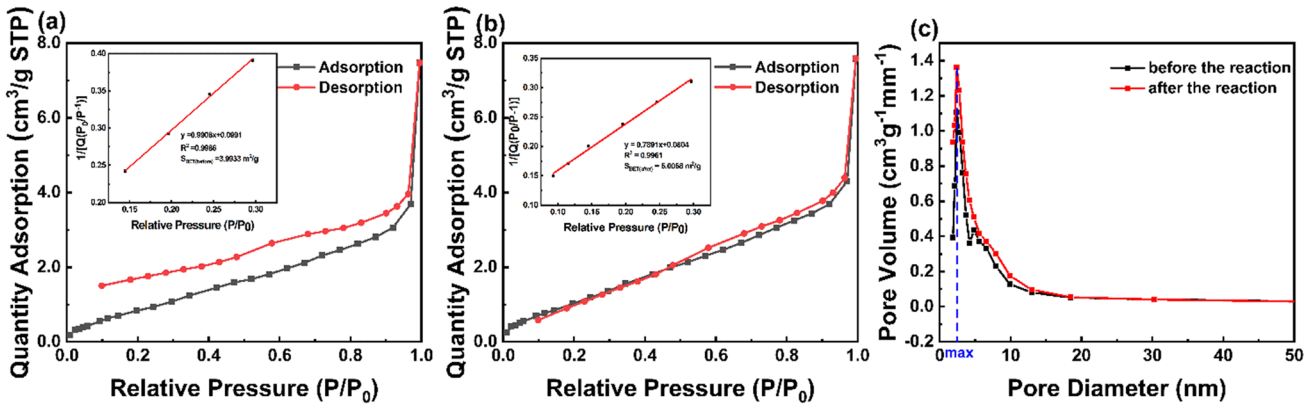

Fig. 2 BET before the reaction (**a**) and after the reaction (**b**), pore size distribution of MBC (**c**)

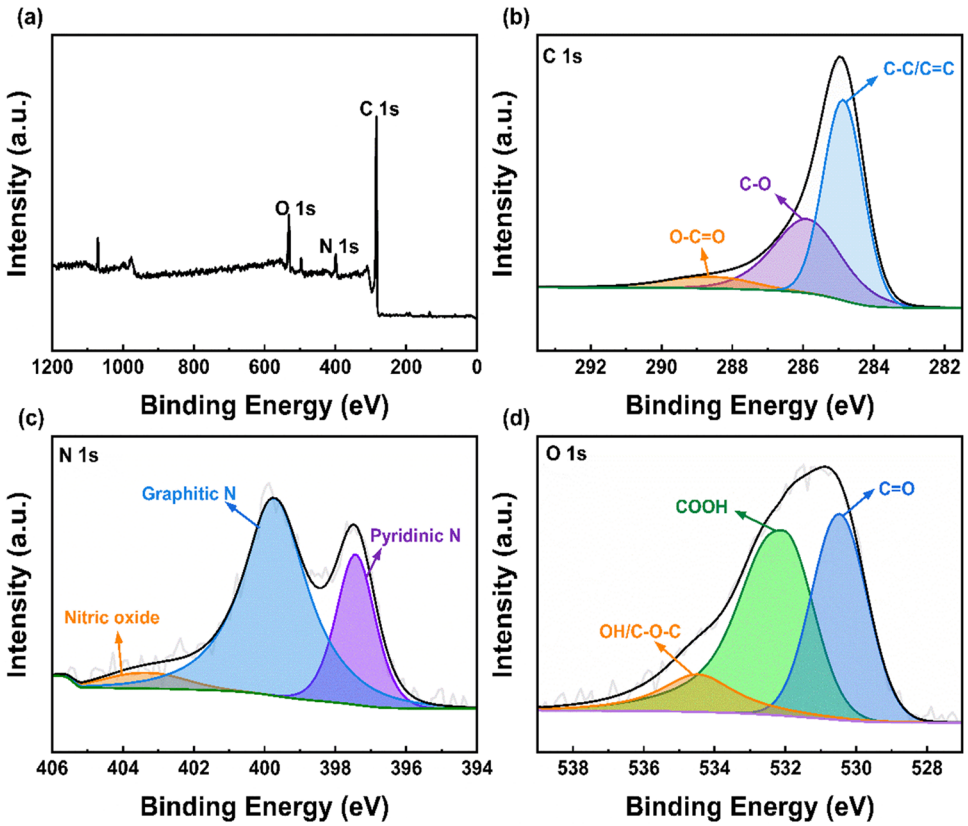

Fig. 3 XPS spectrum of full-scan (**a**), C1s (**b**), N1s (**c**), and O1s (**d**) of MBC

(399.71 eV), and nitric oxide (403.27 eV) (Wang et al. 2021b; Wu et al. 2021b). The presence of N and other heteroatoms could disrupt the original chemical inertness of the carbon layer, producing more defects on the surface and offering more reaction sites for the activation of PS (Chen et al. 2021). The O 1 s of Fig. 3c was fitted by three peaks. The first one was located in the lower binding energy (530.3 eV) and can be attributed to O^{2-}. Two other components were identified as OH-/C–O–C (532.06 eV) and C = O (534.48 eV), respectively (Kong et al. 2016; Wu et al. 2022c; Zhou et al. 2020). Zhao et al. showed that the surface oxygen-containing groups of BC materials, such as carbonyl (C = O), carboxyl (-COOH), and hydroxyl (C-OH) groups, may benefit the catalytic performance of BC (Zhao et al. 2020).

The X-ray diffraction patterns of the samples are shown in Fig. 4a. A broad diffraction peak can be observed at 2θ = 26°, which probably corresponds to the (002) graphitic carbon plane. The broader peak appearing at 2θ = 43° can correspond to the (100) plane of crystalline carbon. It indicated that all samples are amorphous and have an amorphous graphitic carbon structure (Wang et al. 2019a). The diffraction peak at 2θ = 26° indicated parallel stacking and interconnection between the various parts of the graphite

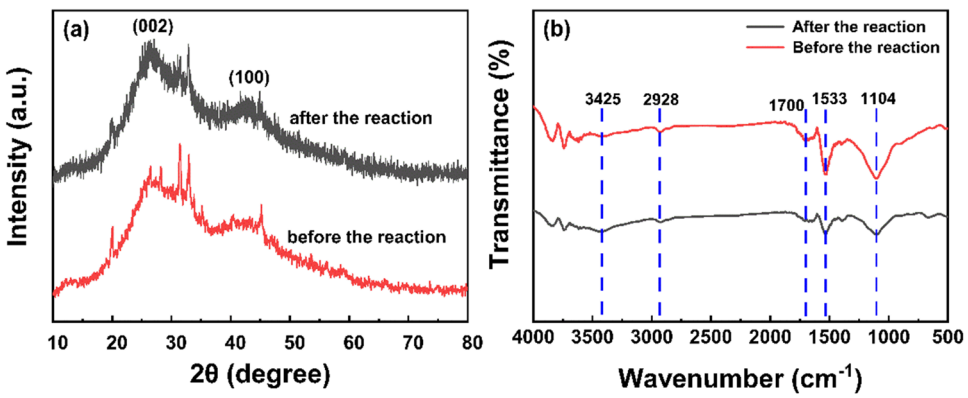

Fig. 4 XRD (**a**) and FTIR spectra (**b**) of MBC before and after the reaction

layers in carbon materials. The diffraction peak at 2θ = 43° showed that sp^2 hybridized carbon atoms interact with each other in the carbon material to create a hexagonal lattice structure (Wang et al. 2021b). In addition, the diffraction peak that appears near 20° represents the graphitized structure (Ding et al. 2021). Two more pronounced diffraction peaks appear near 2θ = 32°, corresponding to the diffraction peaks of (112) and (202) crystal planes of glucuronamide ($C_6H_{11}NO_6$) (Qiao et al. 2016). These diffraction peaks may be due to the carbonization of organic components such as peptidoglycan, lipids, and proteins on the bacterial cell wall (Dik et al. 2018). Fig. 4a revealed that there was no significant variation in the BC samples before and after the reaction, which can indicate the stability of MBC.

FTIR spectroscopy was used to compare the differences in the structure and surface groups of MBC before and after the reaction. As observed in Fig. 4b, five distinct peaks of 3425, 2928, 1700, 1533, and 1104 cm^{-1} appeared in the spectra. The peak around 3425 cm^{-1} is allocated to the stretching vibrations of -OH in phenol functional groups and carboxyl groups (Zhu et al. 2018b). This peak is closely related to the one at 1104 cm^{-1}, due to the symmetric C-O or C-O-C stretching. A peak at 1700 cm^{-1} is caused by the C = O groups (Avramiotis et al. 2021; Guo et al. 2021; Liu et al. 2022b). The bands at 2928 cm^{-1} and 1533 cm^{-1} stand for the stretching vibration of -CH_2- and C = C stretching, respectively (Liu et al. 2016; Rumjit et al. 2021; Sadegh et al. 2021; Wang et al. 2021b). There was a more significant decrease in the peak intensity of MBC at 1100-1700 cm^{-1} after the reaction, which could indicate that these oxygen-containing functional groups play a crucial role in the catalytic degradation (Zhou et al. 2021). The removal capacity of MBC/PS for RhB could be related to the oxygen functional groups (-OH and C = O) in MBC (Xu et al. 2023; Yan et al. 2023).

Evaluation of MBC as the persulfate activator

Fig. 5a compared the removal of RhB by the MBC and MR-1 strains in different systems. It can be observed that 91.7% of RhB could be effectively degraded with the MBC/PS system. However, pure MR-1 almost had no degradation effect and only can remove 50.2% of RhB with PS. The degradation efficiency can be increased by 47.4% with MBC/PS rather than with MR-1/PS. As can be known from Table 1, the conventional ways for using microorganisms to degrade organic pollutants are pure bacteria, bacterial consortia, bacterial film, or bio-electrochemical systems. However, complex reaction systems, rather low degradation efficiency, or a relatively long time consumption of the above

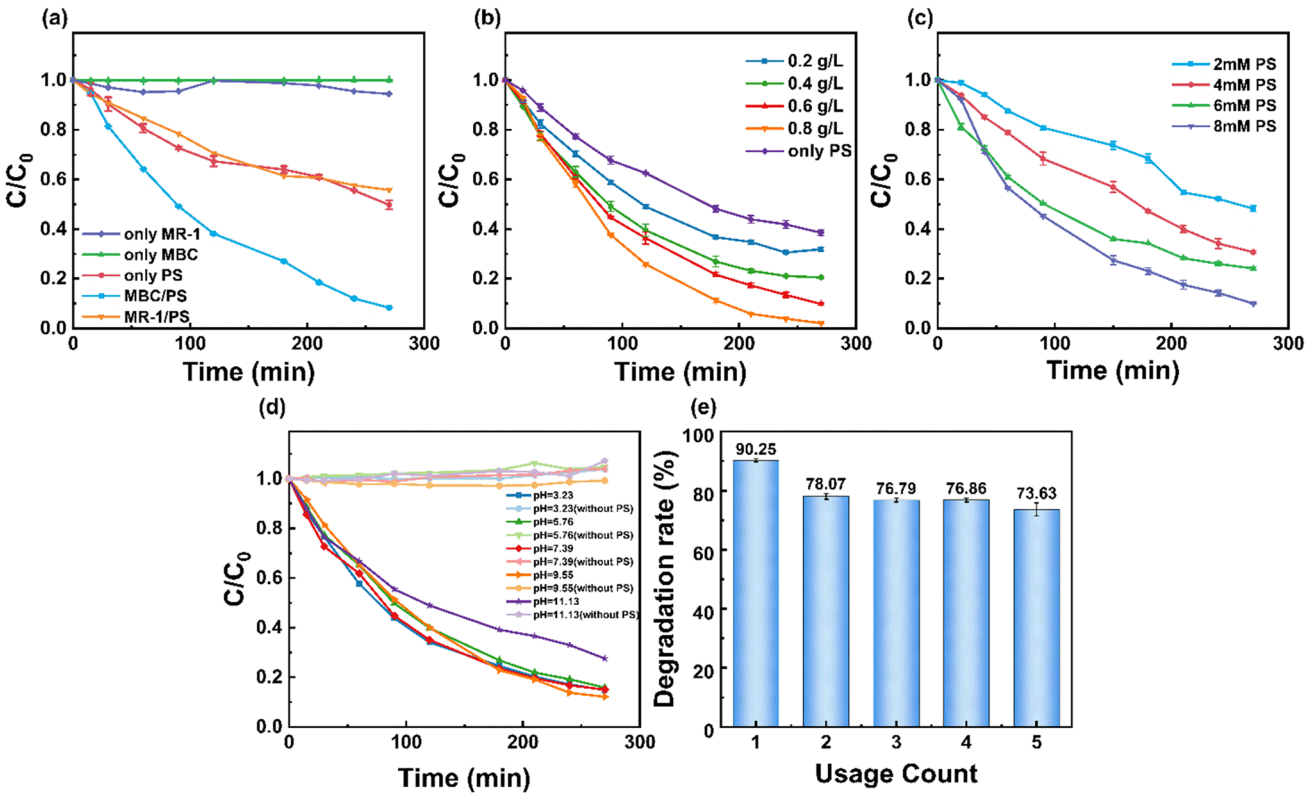

Fig. 5 Degradation of RhB in different systems (**a**) and the effect of catalyst dosage (**b**), PS dosage (**c**), initial pH on RhB removal (C/C_0) by MBC/PS (**d**), and the reusability of MBC (**e**)

Table 1 Comparison of the degradation of organic pollutants by microorganisms in different reaction systems

Bacterial name	Organic pollutants	Reaction system	Maximum degradation	Ref.
White rot fungi	Lignocellulose	Combined bacterial cultures	43.36%	(Chu et al. 2021)
Pseudoarthrobacter sp. and *Gordonia* sp., (PsGo); *Stenotrophomonas* sp., and *Sphingomona* sp. (StSp)	Reactive Black 5	Bacterial consortia strain	85% (for PsGo) 75% (for StSp)	(Eskandari et al. 2019)
Piscibacillus sp. and *Bacillus* sp.	Methanil Yellow G	Halophilic alkalithermophilic bacterial consortium	94%	(Guo et al. 2020)
Enterococcus faecalis and *Klebsiella variicola*	Reactive Red 198	Bacterial consortium	99.26%	(Eslami et al. 2019)
Shewanella oneidensis	Acid Orange 7	Microbial fuel cell (MFC)	80%	(Mani et al. 2019)
Unclassified genus	Reactive Brilliant Red X-3B	Biofilm electrode reactors (BERs)	75.27%	(Cao et al. 2018)
Pseudomonas aeruginosa and *Alcaligenes faecalis*	Polycyclic aromatic hydrocarbons	Bacterial consortium	>80%	(Zhang et al. 2022a)
Bacillus licheniformis ARMP2 and *Pseudomonas aeruginosa* ARMP8	Petroleum hydrocarbons	Bacterial co-culture	88% (ARMP2) 73% (ARMP8)	(Ravi et al. 2022)
Bacillus thuringiensis	Methylene blue	Synergistic effect of enzyme	95%	(Wu et al. 2022a)
MR-1	Rhodamine B	Pure bacteria	44%	This work
MBC		Bacterial-based biochar/PS	91.7%	

ways stimulate some new means to utilize microorganisms. In this work, the MBC was prepared as the PS activator with carbonization of bacteria. Higher degradation efficiency and less degradation time can be achieved with MBC/PS than with MR-1. The oxygen-containing functional groups on the surface of BC such as hydroxyl and carboxyl groups can effectively activate $S_2O_8^{2-}$ to produce $SO_4^{\bullet-}$ (Oh and Nguyen 2022). Furthermore, •OH was also produced due to the hydrolysis of $SO_4^{\bullet-}$. In this work, the pore structure, high N content, and high C = O/C-O ratio of the MBC can provide more catalytic active sites to contribute to the catalytic effect. Therefore, MBC is an effective PS activator that can enhance the ability of PS to remove RhB.

The effect of MBC addition, PS concentration, and initial pH on RhB degradation was assessed in Fig. 5b, d. As shown in Fig. 5b, the degradation efficiency increases with the addition of MBC. One hundred percent of RhB degradation can be achieved with the addition of 0.8 g/L MBC. The k_{obs} reaction rate constant was increased from 0.0046 to 0.0143 min^{-1}, which means that the increase of the catalyst concentration provided more active sites for PS activation (Table 2). PS concentrations also had a significant effect on RhB degradation (Fig. 5c). When the concentration of PS was increased by four times, the removal rate of RhB could be increased by 41.9%. This means that sufficient amount of $SO_4^{\bullet-}$ and •OH need to be produced with the appropriate amount of PS to oxidize and degrade RhB. Initial pH is also usually an important factor in degradation systems. Significant effect of pH values (pH = 3-11) on RhB removal efficiency can be observed in Fig. 5d. Under acidic and neutral conditions, the removal of RhB remained stable at around 88.0% with no obvious changes. However, the removal effect was greatly reduced in strongly alkaline conditions (pH = 11). Such differences may be due to electrostatic adsorption (Shi et al. 2023; Yang et al. 2023). BC has a positively charged surface in acidic solutions, which electrostatically adsorbs the negative ions of PS ($S_2O_8^{2-}$) and readily accesses the surface of the material, enabling effective activation. On the contrary, under alkaline conditions, BC shows more negative charge sites, and the caused electrostatic repulsion may limit its degradation rate. The above experiments show that MBC/PS can effectively degrade RhB over a wide pH range, which also indicates that the degradation reaction conditions are mild and economical and no extra strong acids or alkali are needed.

The reusability and stability of the catalyst MBC were verified by recycling experiments in conjunction with the practical application of the catalyst (Fig. 5e). After five

Table 2 First-order kinetic parameters for degradation of MBC dosage and PS concentration

MBC dosage	$k \times 10^{-3}$ min^{-1}	R^2	PS dosage	$k \times 10^{-3}$ min^{-1}	R^2
0.2 g/L	4.6	0.9678	2 mM	2.8	0.9734
0.4 g/L	6.2	0.9780	4 mM	4.2	0.9865
0.6 g/L	8.6	0.9990	6 mM	5.2	0.9762
0.8 g/L	14.3	0.9930	8 mM	8.4	0.9962

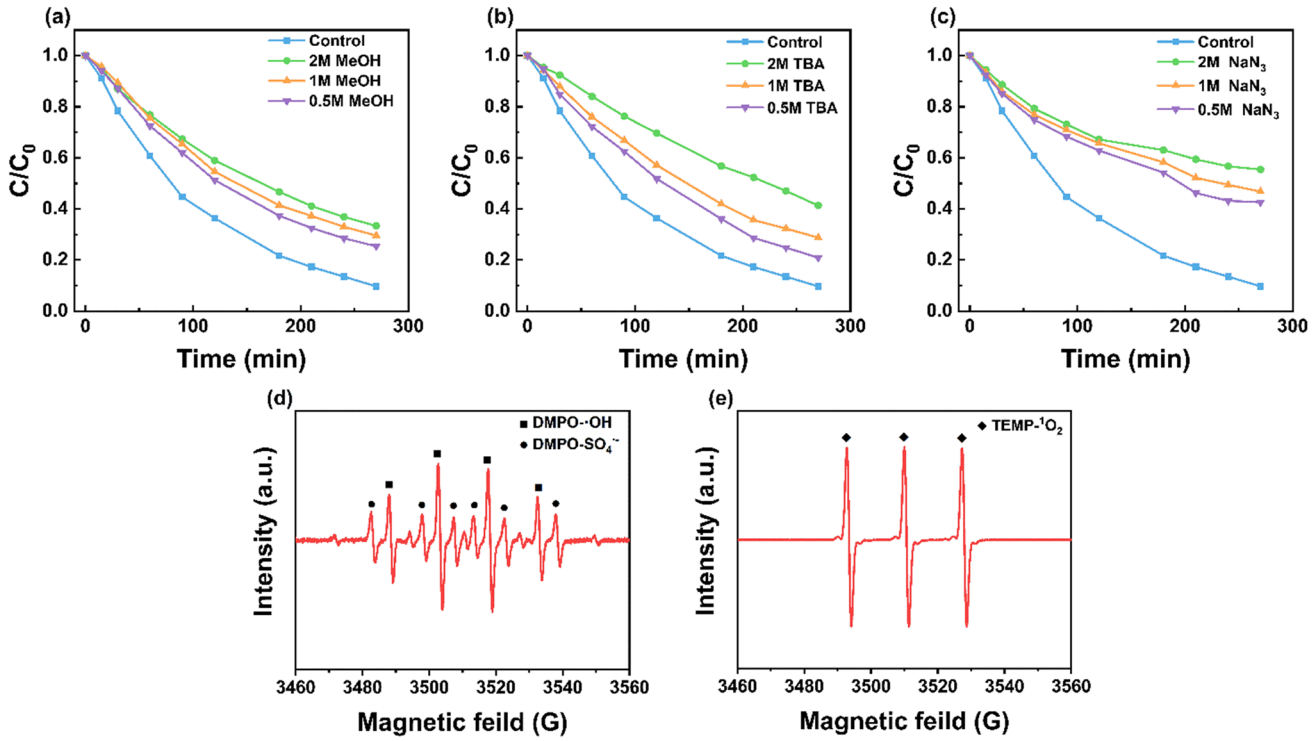

Fig. 6 Effects of free radical inhibitor MeOH (**a**), TBA (**b**), NaN_3 (**c**) on the degradation of RhB by PS catalyzed with MBC and the EPR spectra of •OH and $SO_4^{\bullet-}$ (**d**) and $^1O_2$ (**e**) signals in the MBC/PS system

cycles, it was observed that the removal of RhB decreased by 18.56%, which may be due to the reduction of active sites on the catalyst surface by cleaning and drying processes. In addition, the characterization of the MBC shows that there was no significant change before and after the reaction, which indicates that the material has good structural stability.

Mechanism of persulfate activation by MBC

In general, the oxidation capacity of the catalyst/PS may be ascribed to the generation of free radicals or non-radical active species. Typically, the •OH and $SO_4^{\bullet-}$ were usually regarded as the two major reactants for PS activation by metal-free catalysts. In this work, MeOH, TBA, and NaN_3 were used to investigate the active species of the MBC/PS system. MeOH was highly reactive towards •OH and $SO_4^{\bullet-}$ and could quench both radicals efficiently at different reaction rates ($k_{SO4^{\bullet-}} = 1.1 \times 10^7\ M^{-1}\ s^{-1}$, $k_{\bullet OH} = 9.7 \times 10^8\ M^{-1}\ s^{-1}$) (Guo et al. 2021; He et al. 2021; Wu et al. 2021a; Zhou et al. 2020; Zhu et al. 2018a). TBA can only be used as •OH quencher with a reaction rate of $6 \times 10^8\ M^{-1}\ s^{-1}$, (Hu et al. 2017; Liu et al. 2021; Wu et al. 2021a). Known from Fig. 6a-b, the removal of RhB was decreased by 23.9% and 31.9% after the addition of MeOH and TBA, respectively, which can indicate that both $SO_4^{\bullet-}$ and •OH radicals play a role in the MBC/PS system. However, the inhibition effect of MeOH ($k_{obs-2\ M} = 0.0041\ min^{-1}$) was weaker than that of TBA ($k_{obs-2\ M} = 0.0021\ min^{-1}$) (Table 3), which can confirm that the effect of •OH is more significant than that of $SO_4^{\bullet-}$. The above results can be explained as follows: the compensation effect of $SO_4^{\bullet-}$ produced from PS by CH_2OH• on the degradation efficiency; the affinity of TBA with MBC to prevent from the entry of PS to MBC (Liu et al. 2022a; Ren et al. 2021). Furthermore, it can be found in Fig. 6a-b that MeOH and TBA cannot completely quench the reaction, suggesting that there may be other active species attributed to the RhB removal. NaN_3 was typically used to capture singlet oxygen ($^1O_2$) ($k = 1.2 \times 10^8\ M^{-1}\ s^{-1}$) (Xu et al. 2020), which

Table 3 First-order kinetic parameters for degradation of different quenching agents

MeOH	$k \times 10^{-3}\ min^{-1}$	R^2	TBA	$k \times 10^{-3}\ min^{-1}$	R^2	NaN_3	$k \times 10^{-3}\ min^{-1}$	R^2
0.5 M	5.2	0.9973	0.5 M	5.9	0.9985	0.5 M	3.2	0.9836
1 M	4.7	0.9962	1 M	4.8	0.9983	1 M	2.7	0.9833
2 M	4.1	0.9984	2 M	3.2	0.9983	2 M	2.1	0.9536

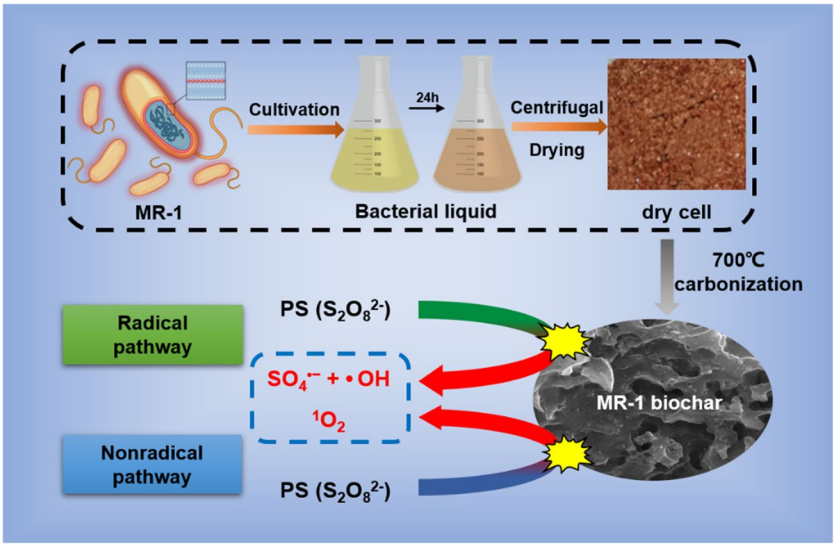

Scheme 1 Schematic representation of the mechanism of MBC activation of persulfate

is the typical active substance in the non-radical pathway. As observed in Fig. 6c, the degradation rate of RhB showed a significant decrease with increasing NaN_3 concentration. 2 M NaN_3 could inhibit the degradation of 46.0% RhB, indicating that $^1O_2$ also played a significant role in RhB degradation by the MBC/PS system.

To further demonstrate the contribution of the active species in the MBC/PS system, an EPR test was performed. •OH or $SO_4^{\bullet-}$ can form stable adducts with DMPO, and $^1O_2$ can be detected by reacting rapidly with TEMP to form $TEMPO^+$ radicals (Wang et al. 2023; Wu et al. 2022b, 2022d). In Fig. 6e, a quadruple peak with a relative intensity ratio of 1:2:2:1 for DMPO-•OH and a six-line peak with a relative intensity ratio of 1:1:1:1:1:1 for the DMPO-$SO_4^{\bullet-}$ adduct can be observed (Wu et al. 2020). Meanwhile, in Fig. 6f, the characteristic signals with the ratio of 1:1:1 for triplet peak of TEMP-$^1O_2$ can be observed (Huang et al. 2023). The results were also verified with the quenching experiments, which demonstrated that the MBC/PS system could indeed catalyze the generation of •OH, $SO_4^{\bullet-}$, and $^1O_2$ from activated PS by the quenching experiments and the EPR measurements. Based on the above experimental results, a more reasonable schematic of MBC activated PS was proposed, as shown in Scheme 1.

Conclusion

In this study, we employed *Shewanella oneidensis* MR-1 for the first time as a raw material for the preparation of biochar for the degradation of RhB by activated PS. Characterization techniques such as SEM, BET, XRD, XPS, and FTIR were used to examine the morphological structure and chemical content of MBC. Meanwhile, by comparing the degradation effects of pure strain MR-1 and MBC, it was discovered that the degradation effect of RhB was significantly improved after the carbonization of the bacterium, proving the high catalytic activity of the MBC material. MBC exhibited good stability and high catalytic action in a wide pH range. The quenching experiments and EPR tests indicated that •OH, $SO_4^{\bullet-}$ and $^1O_2$ play an important role in the MBC/PS system. This study provided a new simple, efficient, and economical catalyst for the activation of PS, and also brings a new perspective on the resource utilization of bacteria.

Author contribution All authors contributed to the study conception and design. Material preparation, data collection, and analysis were performed by Na Yu, Hanyu Ma, Zhihong Wen, Wenbin Zhang, and Jiahao Chen. The manuscript was written primarily by Na Yu, with the rest of the authors providing comments on several versions of the manuscript. All authors read and approved the final manuscript.

Funding This work was financially supported by the National Natural Science Foundation of China (No. 21876032 and 42277023) and the Innovation and Entrepreneurship Training Program for College Students of Guangdong University of Technology (NO. xj2022118450926).

Data availability All data and materials generated or analyzed during this study are included in this published article.

Declarations

Ethics approval Not applicable.

Consent to participate Not applicable.

Consent for publication All the authors are in agreement with the publishment.

Conflict of interest The authors declare no competing interests.

References

Ao X, Sun W, Li S, Yang C, Li C, Lu Z (2019) Degradation of tetracycline by medium pressure UV-activated peroxymonosulfate process: influencing factors, degradation pathways, and toxicity evaluation. Chem Eng J 361:1053–1062. https://doi.org/10.1016/j.cej.2018.12.133

Avramiotis E, Frontistis Z, Manariotis ID, Vakros J, Mantzavinos D (2021) Oxidation of sulfamethoxazole by rice husk biochar-activated persulfate. Catalysts 11:850. https://doi.org/10.3390/catal11070850

Cao X, Wang H, Zhang S, Nishimura O, Li X (2018) Azo dye degradation pathway and bacterial community structure in biofilm electrode reactors. Chemosphere 208:219–225. https://doi.org/10.1016/j.chemosphere.2018.05.190

Chen YP, Zheng CH, Huang YY, Chen YR (2021) Removal of chlortetracycline from water using spent tea leaves-based biochar as adsorption-enhanced persulfate activator. Chemosphere 286:131770. https://doi.org/10.1016/j.chemosphere.2021.131770

Chen X, Guo Z, Liu J, Wu F, Cheng C, Lin H, Ren W, Zhang H (2023) Electron transfer-based peroxydisulfate activation by waste herb residue biochar: adsorption versus surface oxidation. Chem Eng J 451:138560. https://doi.org/10.1016/j.cej.2022.138560

Cheng X, Guo H, Zhang Y, Wu X, Liu Y (2017) Non-photochemical production of singlet oxygen via activation of persulfate by carbon nanotubes. Water Res 113:80–88. https://doi.org/10.1016/j.watres.2017.02.016

Chu X, Awasthi MK, Liu Y, Cheng Q, Qu J, Sun Y (2021) Studies on the degradation of corn straw by combined bacterial cultures. Bioresour Technol 320:124174. https://doi.org/10.1016/j.biortech.2020.124174

Dik DA, Fisher JF, Mobashery S (2018) Cell-wall recycling of the gram-negative bacteria and the nexus to antibiotic resistance. Chem Rev 118:5952–5984. https://doi.org/10.1021/acs.chemrev.8b00277

Ding J, Chen W, Zhang Z, Qin F, Jiang J, He A, Sheng GD (2021) Enhanced removal of cadmium from wastewater with coupled biochar and Bacillus subtilis. Water Sci Technol 83:2075–2086. https://doi.org/10.2166/wst.2021.138

Dong H, Liu W, Zhang H, Zheng X, Duan H, Zhou L, Xu T, Ruan R (2022) Improvement of phosphate solubilizing bacteria Paenibacillus xylanexedens on the growth of Chlorella pyrenoidosa and wastewater treatment in attached cultivation. Chemosphere 306:135604. https://doi.org/10.1016/j.chemosphere.2022.135604

Duan X, Sun H, Ao Z, Zhou L, Wang G, Wang S (2016) Unveiling the active sites of graphene-catalyzed peroxymonosulfate activation. Carbon 107:371–378. https://doi.org/10.1016/j.carbon.2016.06.016

Duan R, Ma S, Xu S, Wang B, He M, Li G, Fu H, Zhao P (2022) Soybean straw biochar activating peroxydisulfate to simultaneously eliminate tetracycline and tetracycline resistance bacteria: insights on the mechanism. Water Res 218:118489. https://doi.org/10.1016/j.watres.2022.118489

Eskandari F, Shahnavaz B, Mashreghi M (2019) Optimization of complete RB-5 azo dye decolorization using novel cold-adapted and mesophilic bacterial consortia. J Environ Manag 241:91–98. https://doi.org/10.1016/j.jenvman.2019.03.125

Eslami H, Shariatifar A, Rafiee E, Shiranian M, Salehi F, Hosseini SS, Eslami G, Ghanbari R, Ebrahimi AA (2019) Decolorization and biodegradation of reactive Red 198 Azo dye by a new Enterococcus faecalis–Klebsiella variicola bacterial consortium isolated from textile wastewater sludge. World J Microbiol Biotechnol 35:38. https://doi.org/10.1007/s11274-019-2608-y

Fan Y, Ji Y, Kong D, Lu J, Zhou Q (2015) Kinetic and mechanistic investigations of the degradation of sulfamethazine in heat-activated persulfate oxidation process. J Hazard Mater 300:39–47. https://doi.org/10.1016/j.jhazmat.2015.06.058

Fang L, Liu K, Li F, Zeng W, Hong Z, Xu L, Shi Q, Ma Y (2021) New insights into stoichiometric efficiency and synergistic mechanism of persulfate activation by zero-valent bimetal (iron/copper) for organic pollutant degradation. J Hazard Mater 403:123669. https://doi.org/10.1016/j.jhazmat.2020.123669

Feng Z, Zhou B, Yuan R, Li H, He P, Wang F, Chen Z, Chen H (2022) Biochar derived from different crop straws as persulfate activator for the degradation of sulfadiazine: influence of biomass types and systemic cause analysis. Chem Eng J 440:135669. https://doi.org/10.1016/j.cej.2022.135669

Forouzesh M, Ebadi A, Aghaeinejad-Meybodi A (2019) Degradation of metronidazole antibiotic in aqueous medium using activated carbon as a persulfate activator. Sep Purif Technol 210:145–151. https://doi.org/10.1016/j.seppur.2018.07.066

Fu J, Feng L, Liu Y, Zhang L, Li S (2021) Electrochemical activation of peroxymonosulfate (PMS) by carbon cloth anode for sulfamethoxazole degradation. Chemosphere 287:132094. https://doi.org/10.1016/j.chemosphere.2021.132094

Guo Z, Ren G, Jiang C, Lu X, Zhu Y, Jiang L, Dai L (2015) High performance heteroatoms quaternary-doped carbon catalysts derived from Shewanella bacteria for oxygen reduction. Sci Rep 5:17064. https://doi.org/10.1038/srep17064

Guo G, Hao J, Tian F, Liu C, Ding K, Zhang C, Yang F, Xu J (2020) Decolorization of Metanil Yellow G by a halophilic alkalithermophilic bacterial consortium. Bioresour Technol 316:123923. https://doi.org/10.1016/j.biortech.2020.123923

Guo Y, Yan L, Li X, Yan T, Song W, Hou T, Tong C, Mu J, Xu M (2021) Goethite/biochar-activated peroxymonosulfate enhances tetracycline degradation: inherent roles of radical and non-radical processes. Sci Total Environ 783:147102. https://doi.org/10.1016/j.scitotenv.2021.147102

Hartshorne RS, Jepson BN, Clarke TA, Field SJ, Fredrickson J, Zachara J, Shi L, Butt JN, Richardson DJ (2007) Characterization of Shewanella oneidensis MtrC: a cell-surface decaheme cytochrome involved in respiratory electron transport to extracellular electron acceptors. J Biol Inorg Chem 12:1083–1094. https://doi.org/10.1007/s00775-007-0278-y

He J, Xiao Y, Tang J, Chen H, Sun H (2019) Persulfate activation with sawdust biochar in aqueous solution by enhanced electron donor-transfer effect. Sci Total Environ 690:768–777. https://doi.org/10.1016/j.scitotenv.2019.07.043

He J, Tang J, Zhang Z, Wang L, Liu Q, Liu X (2021) Magnetic ball-milled FeS@biochar as persulfate activator for degradation of tetracycline. Chem Eng J 404. https://doi.org/10.1016/j.cej.2020.126997

Ho SH, Chen YD, Li R, Zhang C, Ge Y, Cao G, Ma M, Duan X, Wang S, Ren NQ (2019) N-doped graphitic biochars from C-phycocyanin extracted Spirulina residue for catalytic persulfate activation toward nonradical disinfection and organic oxidation. Water Res 159:77–86. https://doi.org/10.1016/j.watres.2019.05.008

Hu P, Su H, Chen Z, Yu C, Li Q, Zhou B, Alvarez PJJ, Long M (2017) Selective degradation of organic pollutants using an efficient metal-free catalyst derived from carbonized polypyrrole via peroxymonosulfate activation. Environ Sci Technol 51:11288–11296. https://doi.org/10.1021/acs.est.7b03014

Huang B-C, Jiang J, Huang G-X, Yu H-Q (2018) Sludge biochar-based catalysts for improved pollutant degradation by activating peroxymonosulfate. J Mater Chem A 6:8978–8985. https://doi.org/10.1039/c8ta02282h

Huang P, Zhang P, Wang C, Du X, Jia H, Sun H (2023) P-doped biochar regulates nZVI nanocracks formation for superefficient persulfate activation. J Hazard Mater 450:130999. https://doi.org/10.1016/j.jhazmat.2023.130999

Kong L, Zhu Y, Liu M, Chang X, Xiong Y, Chen D (2016) Conversion of Fe-rich waste sludge into nano-flake Fe-SC hybrid Fenton-like

catalyst for degradation of AOII. Environ Pollut 216:568–574. https://doi.org/10.1016/j.envpol.2016.06.012

Lai C, Huang F, Zeng G, Huang D, Qin L, Cheng M, Zhang C, Li B, Yi H, Liu S, Li L, Chen L (2019a) Fabrication of novel magnetic MnFe2O4/bio-char composite and heterogeneous photo-Fenton degradation of tetracycline in near neutral pH. Chemosphere 224:910–921. https://doi.org/10.1016/j.chemosphere.2019.02.193

Lai C, Zhang M, Li B, Huang D, Zeng G, Qin L, Liu X, Yi H, Cheng M, Li L, Chen Z, Chen L (2019b) Fabrication of CuS/BiVO4 (0 4 0) binary heterojunction photocatalysts with enhanced photocatalytic activity for ciprofloxacin degradation and mechanism insight. Chem Eng J 358:891–902. https://doi.org/10.1016/j.cej.2018.10.072

Levanov AV, Isaikina OY, Gasanova RB, Uzhel AS, Lunin VV (2019) Kinetics of chlorate formation during ozonation of aqueous chloride solutions. Chemosphere 229:68–76. https://doi.org/10.1016/j.chemosphere.2019.04.105

Li B, Lai C, Zeng G, Qin L, Yi H, Huang D, Zhou C, Liu X, Cheng M, Xu P, Zhang C, Huang F, Liu S (2018) Facile hydrothermal synthesis of Z-scheme Bi2Fe4O9/Bi2WO6 heterojunction photocatalyst with enhanced visible light photocatalytic activity. ACS Appl Mater Interfaces 10:18824–18836. https://doi.org/10.1021/acsami.8b06128

Li K, Xu S, Liu X, Li H, Zhan S, Ma S, Huang Y, Liu S, Zhuang X (2022) The organic contaminants degradation in Mn-NRGO and peroxymonosulfate system: the significant synergistic effect between Mn nanoparticles and doped nitrogen. Chem Eng J 438. https://doi.org/10.1016/j.cej.2022.135630

Liang J, Xu X, Qamar Zaman W, Hu X, Zhao L, Qiu H, Cao X (2019) Different mechanisms between biochar and activated carbon for the persulfate catalytic degradation of sulfamethoxazole: roles of radicals in solution or solid phase. Chem Eng J 375. https://doi.org/10.1016/j.cej.2019.121908

Liu XQ, Ding HS, Wang YY, Liu WJ, Jiang H (2016) Pyrolytic temperature dependent and ash catalyzed formation of sludge char with ultra-high adsorption to 1-naphthol. Environ Sci Technol 50:2602–2609. https://doi.org/10.1021/acs.est.5b04536

Liu H, Liu Y, Tang L, Wang J, Yu J, Zhang H, Yu M, Zou J, Xie Q (2020) Egg shell biochar-based green catalysts for the removal of organic pollutants by activating persulfate. Sci Total Environ 745:141095. https://doi.org/10.1016/j.scitotenv.2020.141095

Liu H, Wang C, Wang G (2020b) Photocatalytic advanced oxidation processes for water treatment: recent advances and perspective. ChemAsian J 15:3239–3253. https://doi.org/10.1002/asia.202000895

Liu D, Li Q, Hou J, Zhao H (2021) Mixed-valent manganese oxide for catalytic oxidation of orange II by activation of persulfate: heterojunction dependence and mechanism. Catal Sci Technol 11:3715–3723. https://doi.org/10.1039/d1cy00087j

Liu F, Ding J, Zhao G, Zhao Q, Wang K, Wang G, Gao Q (2022) Catalytic pyrolysis of lotus leaves for producing nitrogen self-doping layered graphitic biochar: performance and mechanism for peroxydisulfate activation. Chemosphere 302:134868. https://doi.org/10.1016/j.chemosphere.2022.134868

Liu S, Lai C, Li B, Liu X, Zhou X, Zhang C, Qin L, Li L, Zhang M, Yi H, Fu Y, Yan H, Chen L (2022b) Heteroatom doping in metal-free carbonaceous materials for the enhancement of persulfate activation. Chem Eng J 427. https://doi.org/10.1016/j.cej.2021.131655

Lu X, Shao Y, Gao N, Chen J, Zhang Y, Xiang H, Guo Y (2017) Degradation of diclofenac by UV-activated persulfate process: kinetic studies, degradation pathways and toxicity assessments. Ecotoxicol Environ Saf 141:139–147. https://doi.org/10.1016/j.ecoenv.2017.03.022

Mani P, Fidal VT, Bowman K, Breheny M, Chandra TS, Keshavarz T, Kyazze G (2019) Degradation of azo dye (acid orange 7) in a microbial fuel cell: comparison between anodic microbial-mediated reduction and cathodic laccase-mediated oxidation. Front Energy Res 7. https://doi.org/10.3389/fenrg.2019.00101

Milh H, Cabooter D, Dewil R (2021) Role of process parameters in the degradation of sulfamethoxazole by heat-activated peroxymonosulfate oxidation: radical identification and elucidation of the degradation mechanism. Chem Eng J 422. https://doi.org/10.1016/j.cej.2021.130457

Monteagudo JM, El-Taliawy H, Duran A, Caro G, Bester K (2018) Sono-activated persulfate oxidation of diclofenac: degradation, kinetics, pathway and contribution of the different radicals involved. J Hazard Mater 357:457–465. https://doi.org/10.1016/j.jhazmat.2018.06.031

Nasseri S, Mahvi AH, Seyedsalehi M, Yaghmaeian K, Nabizadeh R, Alimohammadi M, Safari GH (2017) Degradation kinetics of tetracycline in aqueous solutions using peroxydisulfate activated by ultrasound irradiation: effect of radical scavenger and water matrix. J Mol Liq 241:704–714. https://doi.org/10.1016/j.molliq.2017.05.137

Oh SY, Nguyen THA (2022) Ozonation of phenol in the presence of biochar and carbonaceous materials: the effect of surface functional groups and graphitic structure on the formation of reactive oxygen species. J Environ Chem Eng 10:107386. https://doi.org/10.1016/j.jece.2022.107386

Oh SY, Kim HW, Park JM, Park HS, Yoon C (2009) Oxidation of polyvinyl alcohol by persulfate activated with heat, Fe2+, and zero-valent iron. J Hazard Mater 168:346–351. https://doi.org/10.1016/j.jhazmat.2009.02.065

Ouyang D, Chen Y, Yan J, Qian L, Han L, Chen M (2019) Activation mechanism of peroxymonosulfate by biochar for catalytic degradation of 1,4-dioxane: important role of biochar defect structures. Chem Eng J 370:614–624. https://doi.org/10.1016/j.cej.2019.03.235

Qiao Y, Wang H, Zhang X, Jia P, Shen T, Hao X, Tang Y, Wang X, Gao W, Kong L (2016) Ultrahigh volumetric capacitance biomorphic porous carbon material derived from mold. Mater Lett 184:252–256. https://doi.org/10.1016/j.matlet.2016.08.081

Qin L, Zeng Z, Zeng G, Lai C, Duan A, Xiao R, Huang D, Fu Y, Yi H, Li B, Liu X, Liu S, Zhang M, Jiang D (2019) Cooperative catalytic performance of bimetallic Ni-Au nanocatalyst for highly efficient hydrogenation of nitroaromatics and corresponding mechanism insight. Appl Catal B-Environ 259. https://doi.org/10.1016/j.apcatb.2019.118035

Ravi A, Ravuri M, Krishnan R, Narenkumar J, Anu K, Alsalhi MS, Devanesan S, Kamala-Kannan S, Rajasekar A (2022) Characterization of petroleum degrading bacteria and its optimization conditions on effective utilization of petroleum hydrocarbons. Microbiol Res 265:127184. https://doi.org/10.1016/j.micres.2022.127184

Ren X, Wang J, Yu J, Song B, Feng H, Shen M, Zhang H, Zou J, Zeng G, Tang L, Wang J (2021) Waste valorization: transforming the fishbone biowaste into biochar as an efficient persulfate catalyst for degradation of organic pollutant. J Clean Prod 291:125225. https://doi.org/10.1016/j.jclepro.2020.125225

Rumjit NP, Samsudin NA, Low FW, Thomas P, Lai CW, Velayudhaperumal Chellam P, Bin Johan MR, Lim Y-C, Amin N, Tiong SK (2021) Kinetic and isotherm studies on adsorptive removal of sulfates by cotton shell derived biochar: recovery of sulfates from marcasite soil. Sustain Chem Pharm 20. https://doi.org/10.1016/j.scp.2020.100361

Sadegh N, Haddadi H, Arabkhani P, Asfaram A, Sadegh F (2021) Simultaneous elimination of rhodamine B and malachite green dyes from the aqueous sample with magnetic reduced graphene oxide nanocomposite: Optimization using experimental design. J Mol Liq 343. https://doi.org/10.1016/j.molliq.2021.117710

Sanz C, Casadoi M, Tadic Đ, Pastor-López EJ, Navarro-Martin L, Parera J, Tugues J, Ortiz CA, Bayona JM, Piña B (2022) Impact

of organic soil amendments in antibiotic levels, antibiotic resistance gene loads, and microbiome composition in corn fields and crops. Environ Res 214:113760. https://doi.org/10.1016/j.envres.2022.113760

Shi C, Li Y, Feng H, Jia S, Xue R, Li G, Wang G (2017) Removal of p-nitrophenol using persulfate activated by biochars prepared from different biomass materials. Chem Res Chinese U 34:39–43. https://doi.org/10.1007/s40242-017-7245-0

Shi C, Nie L, Hu K, Zheng C, Xu C, Song H, Wang G (2023) New insights into peroxydisulfate activation by nanostructured and bulky carbons. Appl Catal B-Environ 325:122371. https://doi.org/10.1016/j.apcatb.2023.122371

Si P, Li J, Xie W, Dong H, Qiang Z (2021) Deciphering nitrogen removal mechanism through marine anammox bacteria treating nitrogen-laden saline wastewater under various phosphate doses: microbial community shift and phosphate crystal. Bioresour Technol 325:124707. https://doi.org/10.1016/j.biortech.2021.124707

Sun W, Chen L, Wang J (2017) Degradation of PVA (polyvinyl alcohol) in wastewater by advanced oxidation processes. J Adv Oxid Technol 20. https://doi.org/10.1515/jaots-2017-0018

Tag AT, Duman G, Ucar S, Yanik J (2016) Effects of feedstock type and pyrolysis temperature on potential applications of biochar. J Anal Appl Pyrol 120:200–206. https://doi.org/10.1016/j.jaap.2016.05.006

Tang X, Ma S, Xu S, Yang Q, Huang Y, Wang J, Hua D (2023) Effects of different pretreatment strategies during porous carbonaceous materials fabrication on their peroxydisulfate activation for organic pollutant degradation: focus on mechanism. Chem Eng J 451. https://doi.org/10.1016/j.cej.2022.138576

Timmis K, Hallsworth JE (2022) The darkest microbiome—a posthuman biosphere. Microb Biotechnol 15:176–185. https://doi.org/10.1111/1751-7915.13976

Wacławek S, Lutze HV, Grübel K, Padil VVT, Černík M, Dionysiou DD (2017) Chemistry of persulfates in water and wastewater treatment: a review. Chem Eng J 330:44–62. https://doi.org/10.1016/j.cej.2017.07.132

Wang S, Wang J (2019) Activation of peroxymonosulfate by sludge-derived biochar for the degradation of triclosan in water and wastewater. Chem Eng J 356:350–358. https://doi.org/10.1016/j.cej.2018.09.062

Wang B, Li YN, Wang L (2019a) Metal-free activation of persulfates by corn stalk biochar for the degradation of antibiotic norfloxacin: activation factors and degradation mechanism. Chemosphere 237:124454. https://doi.org/10.1016/j.chemosphere.2019.124454

Wang C, Chen W, Yang L, Wei R, Ni J, Yang Y (2019b) Insights into the roles of the morphological carbon structure and ash in the sorption of aromatic compounds to wood-derived biochars. Sci Total Environ 693:133455. https://doi.org/10.1016/j.scitotenv.2019.07.261

Wang B, Deng C, Ma W, Sun Y (2021a) Modified nanoscale zero-valent iron in persulfate activation for organic pollution remediation: a review. Environ Sci Pollut Res Int 28:34229–34247. https://doi.org/10.1007/s11356-021-13972-w

Wang Z, Huang L, Wang Y, Chen X, Ren H (2021b) Activation of peroxymonosulfate using metal-free in situ N-doped carbonized polypyrrole: a non-radical process. Environ Res 193:110537. https://doi.org/10.1016/j.envres.2020.110537

Wang J, Wang S (2021) Toxicity changes of wastewater during various advanced oxidation processes treatment: an overview. J Clean Prod 315. https://doi.org/10.1016/j.jclepro.2021.128202

Wang Y, Lin Y, Yang C, Wu S, Fu X, Li X (2023) Calcination temperature regulates non-radical pathways of peroxymonosulfate activation via carbon catalysts doped by iron and nitrogen. Chem Eng J 451. https://doi.org/10.1016/j.cej.2022.138468

Wei L, Karahan HE, Goh K, Jiang W, Yu D, Birer Ö, Jiang R, Chen Y (2015a) A high-performance metal-free hydrogen-evolution reaction electrocatalyst from bacterium derived carbon. J Mater Chem A 3:7210–7214. https://doi.org/10.1039/c5ta00966a

Wei L, Yu D, Karahan HE, Birer Ö, Goh K, Yuan Y, Jiang W, Liang W, Chen Y (2015b) E. coli-derived carbon with nitrogen and phosphorus dual functionalities for oxygen reduction reaction. Catal Today 249:228–235. https://doi.org/10.1016/j.cattod.2014.08.031

Wei X, Gao N, Li C, Deng Y, Zhou S, Li L (2016) Zero-valent iron (ZVI) activation of persulfate (PS) for oxidation of bentazon in water. Chem Eng J 285:660–670. https://doi.org/10.1016/j.cej.2015.08.120

Wu Y, Guo J, Han Y, Zhu J, Zhou L, Lan Y (2018) Insights into the mechanism of persulfate activated by rice straw biochar for the degradation of aniline. Chemosphere 200:373–379. https://doi.org/10.1016/j.chemosphere.2018.02.110

Wu W, Zhu S, Huang X, Wei W, Jin C, Ni BJ (2021a) Determination of instinct components of biomass on the generation of persistent free radicals (PFRs) as critical redox sites in pyrogenic chars for persulfate activation. Environ Sci Technol 55:7690–7701. https://doi.org/10.1021/acs.est.1c01882

Wu W, Zhu S, Huang X, Wei W, Ni BJ (2021b) Mechanisms of persulfate activation on biochar derived from two different sludges: dominance of their intrinsic compositions. J Hazard Mater 408:124454. https://doi.org/10.1016/j.jhazmat.2020.124454

Wu K, Shi M, Pan X, Zhang J, Zhang X, Shen T, Tian Y (2022a) Decolourization and biodegradation of methylene blue dye by a ligninolytic enzyme-producing Bacillus thuringiensis: degradation products and pathway. Enzyme Microb Technol 156:109999. https://doi.org/10.1016/j.enzmictec.2022.109999

Wu L, Li Z, Cheng P, She Y, Wang W, Tian Y, Ma J, Sun Z (2022b) Efficient activation of peracetic acid by mixed sludge derived biochar: critical role of persistent free radicals. Water Res 223:119013. https://doi.org/10.1016/j.watres.2022.119013

Wu S, Cai X, Liao Z, He W, Shen J, Yuan Y, Ning X (2022c) Redox properties of nano-sized biochar derived from wheat straw biochar. RSC Adv 12:11039–11046. https://doi.org/10.1039/d2ra01211a

Wu S, Yang C, Lin Y, Cheng JJ (2022d) Efficient degradation of tetracycline by singlet oxygen-dominated peroxymonosulfate activation with magnetic nitrogen-doped porous carbon. J Environ Sci (china) 115:330–340. https://doi.org/10.1016/j.jes.2021.08.002

Wu Y, Zhu X, Wang X, Lin Z, Reinfelder JR, Li F, Liu T (2023) A new electron shuttling pathway mediated by lipophilic phenoxazine via the interaction with periplasmic and inner membrane proteins of Shewanella oneidensis MR-1. Environ Sci Technol 57:2636–2646. https://doi.org/10.1021/acs.est.2c07862

Wu S, Liu H, Yang C, Li X, Lin Y, Yin K, Sun J, Teng Q, Du C, Zhong Y (2020) High-performance porous carbon catalysts doped by iron and nitrogen for degradation of bisphenol F via peroxymonosulfate activation. Chem Eng J 392. https://doi.org/10.1016/j.cej.2019.123683

Xu L, Ye Z, Pan Y, Zhang Y, Gong H, Mei X, Qiao W, Gan L (2023) Effect of lignocellulosic biomass composition on the performance of biochar for the activation of peroxymonosulfate to degrade diclofenac. Sep Purif Technol 311:123312. https://doi.org/10.1016/j.seppur.2023.123312

Xu L, Wu C, Liu P, Bai X, Du X, Jin P, Yang L, Jin X, Shi X, Wang Y (2020) Peroxymonosulfate activation by nitrogen-doped biochar from sawdust for the efficient degradation of organic pollutants. Chem Eng J 387. https://doi.org/10.1016/j.cej.2020.124065

Yan Y, Yang J, Zhu R, Nie Y, Jin B, Li S (2020) Performance evaluation and microbial community analysis of the composite filler

micro-embedded with Pseudomonas putida for the biodegradation of toluene. Process Biochem 92:10–16. https://doi.org/10.1016/j.procbio.2020.02.027

Yan J, Gong L, Chai S, Guo C, Zhang W, Wan H (2023) ZIF-67 loaded lotus leaf-derived biochar for efficient peroxymonosulfate activation for sustained levofloxacin degradation. Chem Eng J 458:141456. https://doi.org/10.1016/j.cej.2023.141456

Yang Z, Wang X-l, Li H, Yang J, Zhou L-Y, Liu Y-d (2017) Reactivation of aged-ZVI by iron-reducing bacterium Shewanella putrefaciens for enhanced reductive dechlorination of trichloroethylene. J Chem Technol Biot 92:2642–2649. https://doi.org/10.1002/jctb.5284

Yang H, Qiu R, Tang Y, Ye S, Wu S, Qin F, Xiang L, Tan X, Zeng G, Yan M (2023) Carbonyl and defect of metal-free char trigger electron transfer and O2•− in persulfate activation for Aniline aerofloat degradation. Water Res 231:119659. https://doi.org/10.1016/j.watres.2023.119659

Yin R, Guo W, Wang H, Du J, Wu Q, Chang J-S, Ren N (2019) Singlet oxygen-dominated peroxydisulfate activation by sludge-derived biochar for sulfamethoxazole degradation through a nonradical oxidation pathway: performance and mechanism. Chem Eng J 357:589–599. https://doi.org/10.1016/j.cej.2018.09.184

Yu J, Feng H, Tang L, Pang Y, Zeng G, Lu Y, Dong H, Wang J, Liu Y, Feng C, Wang J, Peng B, Ye S (2020) Metal-free carbon materials for persulfate-based advanced oxidation process: microstructure, property and tailoring. Prog Mater Sci 111. https://doi.org/10.1016/j.pmatsci.2020.100654

Zeenat, Elahi A, Bukhari DA, Shamim S, Rehman A (2021) Plastics degradation by microbes: a sustainable approach. J King Saud Univ-Sci 33:101538. https://doi.org/10.1016/j.jksus.2021.101538

Zeng G, Yang R, Fu X, Zhou Z, Xu Z, Zhou Z, Qiu Z, Sui Q, Lyu S (2021) Naphthalene degradation in aqueous solution by Fe(II) activated persulfate coupled with citric acid. Sep Purif Technol 264. https://doi.org/10.1016/j.seppur.2021.118441

Zhang M, Dale JR, DiChristina TJ, Stack AG (2009) Dissolution morphology of iron (Oxy)(Hydr)Oxides exposed to the dissimilatory iron-reducing bacteriumShewanella oneidensisMR-1. Geomicrobiol J 26:83–92. https://doi.org/10.1080/01490450802660565

Zhang S, Deng X, Chen A, Zhou H, Xie Z, Liang Y, Zeng F (2019a) Facile synthesis of Pd supported on Shewanella as an efficient catalyst for oxygen reduction reaction. Int J Hydrogen Energ 44:21759–21768. https://doi.org/10.1016/j.ijhydene.2019.06.141

Zhang Y, Yuan X, Lu W, Yan Y, Zhu J, Chou T-W (2019b) MnO2 based sandwich structure electrode for supercapacitor with large voltage window and high mass loading. Chem Eng J 368:525–532. https://doi.org/10.1016/j.cej.2019.02.206

Zhang S, Li Q, Zhou H, Xuan W, Liang Y, Xie Z, Liu F (2021) Scalable preparation of Pd/bacteria-rGO(CNT, Ketjen) composites for efficient oxygen reduction catalyst. Int J Hydrogen Energ 46:5664–5676. https://doi.org/10.1016/j.ijhydene.2020.11.075

Zhang L, Yang B, Qu C, Chen G, Qi F, Yu T, Mustapha A (2022a) Construction and degradation performance study of polycyclic aromatic hydrocarbons (PAHs) degrading bacterium consortium. Appl Sci 12:2354. https://doi.org/10.3390/app12052354

Zhang S, Zhou H, Liao H, Tan P, Tian W, Pan J (2022b) Microbial synthesis of efficient palladium electrocatalyst with high loadings for oxygen reduction reaction in acidic medium. J Colloid Interface Sci 611:161–171. https://doi.org/10.1016/j.jcis.2021.12.080

Zhao C, Ma J, Li Z, Xia H, Liu H, Yang Y (2020) Highly enhanced adsorption performance of tetracycline antibiotics on KOH-activated biochar derived from reed plants. RSC Adv 10:5066–5076. https://doi.org/10.1039/c9ra09208k

Zhao Y, Dai H, Ji J, Yuan X, Li X, Jiang L, Wang H (2022) Resource utilization of luffa sponge to produce biochar for effective degradation of organic contaminants through persulfate activation. Sep Purif Technol 288:120650. https://doi.org/10.1016/j.seppur.2022.120650

Zhou X, Lai C, Huang D, Zeng G, Chen L, Qin L, Xu P, Cheng M, Huang C, Zhang C, Zhou C (2018) Preparation of water-compatible molecularly imprinted thiol-functionalized activated titanium dioxide: Selective adsorption and efficient photodegradation of 2, 4-dinitrophenol in aqueous solution. J Hazard Mater 346:113–123. https://doi.org/10.1016/j.jhazmat.2017.12.032

Zhou S, Zhou L, Zhang Y, Sun J, Wen J, Yuan Y (2019) Upgrading earth-abundant biomass into three-dimensional carbon materials for energy and environmental applications. J Mater Chem A 7:4217–4229. https://doi.org/10.1039/c8ta12159a

Zhou X, Zeng Z, Zeng G, Lai C, Xiao R, Liu S, Huang D, Qin L, Liu X, Li B, Yi H, Fu Y, Li L, Zhang M, Wang Z (2020) Insight into the mechanism of persulfate activated by bone char: unraveling the role of functional structure of biochar. Chem Eng J 401. https://doi.org/10.1016/j.cej.2020.126127

Zhou X, Zhu Y, Niu Q, Zeng G, Lai C, Liu S, Huang D, Qin L, Liu X, Li B, Yi H, Fu Y, Li L, Zhang M, Zhou C, Liu J (2021) New notion of biochar: a review on the mechanism of biochar applications in advannced oxidation processes. Chem Eng J 416. https://doi.org/10.1016/j.cej.2021.129027

Zhu H, Yin J, Wang XL, Wang HY, Yang XR (2013) Microorganism-derived heteroatom-doped carbon materials for oxygen reduction and supercapacitors. Adv Func Mater 23:1305–1312. https://doi.org/10.1002/adfm.201201643

Zhu C, Zhu F, Liu C, Chen N, Zhou D, Fang G, Gao J (2018a) Reductive hexachloroethane degradation by S2O8(*-) with thermal activation of persulfate under anaerobic conditions. Environ Sci Technol 52:8548–8557. https://doi.org/10.1021/acs.est.7b06279

Zhu F, Ma S, Liu T, Deng X (2018b) Green synthesis of nano zerovalent iron/Cu by green tea to remove hexavalent chromium from groundwater. J Clean Prod 174:184–190. https://doi.org/10.1016/j.jclepro.2017.10.302

Zhu Q, Guo K, Ma S, Wang S, Tang X, Duan R, Huang Y, Wang J, Cheng G, Xu S, Zhuang X (2023) Sulfadiazine oxidation by peroxodisulfate and cobalt loaded graphitic biochar system: the dominant role of graphitic domain. Chem Eng J 455. https://doi.org/10.1016/j.cej.2022.140744